Control Engineering Practice 17 (2009) 974–983

Contents lists available at ScienceDirect

Control Engineering Practice

journal homepage: www.elsevier.com/locate/conengprac

Randomization-based control design for Mini-UAVs

Laura Lorefice [a], Barbara Pralio [b], Roberto Tempo [c,*]

[a] Engineering and Design—Aerodynamics, Fiat Group Automobiles, Torino, Italy
[b] Department of Production Systems and Business Economics, Politecnico di Torino, Torino, Italy
[c] IEIIT-CNR, Politecnico di Torino, Torino, Italy

ARTICLE INFO

Article history:
Received 7 March 2008
Accepted 3 March 2009
Available online 18 April 2009

Keywords:
Mini-UAVs
Flight control systems
Uncertain parameters
Robustness
Randomized algorithms

ABSTRACT

The area of research on probabilistic and randomized methods for analysis and design of uncertain systems is fairly recent and is focused both on algorithmic as well as theoretical developments. In this paper a framework for randomization-based control design is presented and applied to a Mini-UAV platform. The proposed approach makes use of random search and uncertainty randomization for controller synthesis and probabilistic robustness analysis. Several structured uncertain parameters, related to the plant and to the operating conditions, are taken into account to design a robust flight control system. A selection criterion, based on estimated probability and its degradation function, is proposed in order to match stability and performance metrics fulfillment. Computational issues associated to the specific application, integration of a priori domain knowledge and human designer interaction with automated design are also addressed.

1. Introduction

In the last decade, the acronym MAVs (micro-aerial vehicles) has been used to define flying objects characterized by physical size approximately smaller than 6 in, in length, width or height. Recalling a classical definition, see, e.g. Davis (1996), these flying objects can be considered as "aerial robots, as six degrees-of-freedom machines whose mobility can deploy a useful micropayload to a remote, or otherwise hazardous location, where it may perform any of a variety of missions." The concept of unmanned aerial vehicles (UAVs) of reduced dimensions, able to perform mission profiles not compatible with any existing piloted platforms, has been subsequently extended to bigger systems and it now incorporates the so-called Mini-UAVs, having maximum dimension up to 6 ft. A large number of successful designs have been performed for either research, commercial or military purposes by several universities, industries and government-funded agencies both in the US as well as in Europe. In fact, recently UAVs have been the subject of considerable interest and development within the systems and control community, see, e.g. Dobrokhodov, Kaminer, Jones, and Reza (2006), Elgersma, Ganguli, Ha, and Samad (2004), Keviczky and Balas (2005), Redding, McLain, Beard, and Taylor (2006), Campa et al. (2007) and Peddle, Jones, and Treurnicht (2009).

The sensitivity to changes in flight conditions, the assumptions related to the aerodynamic model, the inaccuracies in geometric and inertial data represent a possible set of uncertainties in plant and environment modeling. Therefore, the design of a robust flight control system which guarantees a suitable level of tolerance to environmental changes and platform manufacturing/modeling inaccuracies plays a key role whenever stability and performance requirements have to be fulfilled (see Lombaerts, Mulder, Voorsluijs, & Decupyere, 2005).

Classical techniques such as, for example, μ-theory, see Zhou, Doyle, and Glover (1996), and linear-parameter varying (LVP), see Lu and Wu (2006) and Fujisaki, Dabbene, and Tempo (2003), have been frequently used for aircraft control design. However, the platform herein considered is affected by uncertainty of parametric type, which enters nonlinearly into the model, and standard robustness tools proposed in the literature, see, e.g. Barmish (1994), are often not effective in this case. In addition, the mathematical model under attention is obtained by numerical linearization of the full order nonlinear system representing the aircraft dynamics, so that explicit relationships between the state-space matrices and the uncertain parameters are not available. Concerning this, it has to be noted that the linearization procedure needs to be repeated whenever the values of the uncertain parameters change. For these reasons, the present paper proposes a different innovative approach to control design, referring to randomization for gain synthesis as well as for closed-loop system analysis. This approach makes use of random search and uncertainty randomization for controller synthesis and probabilistic robustness analysis. It is based on the theory of *randomized algorithms*, see Tempo, Calafiore, and Dabbene (2005), and on statistical learning theory which aims at deriving uniform laws of large numbers, see Vidyasagar (1998) and Vidyasagar and Blondel

* Corresponding author.
E-mail address: tempo@polito.it (R. Tempo).

0967-0661/$ - see front matter © 2009 Elsevier Ltd. All rights reserved.
doi:10.1016/j.conengprac.2009.03.003

(2001). These algorithms are easy to implement and they have low computational complexity, which depends on the two probabilistic parameters, *accuracy* and *confidence*. Moreover, the obtained robustness bounds are generally less conservative than the classical ones, obviously at the expense of a probabilistic risk of failure.

The theory of randomized algorithms follows the line of research that was initiated in the early eighties, see Stengel (1980). In this and several subsequent papers, see, e.g. Ray and Stengel (1993) and Wang and Stengel (2005, 2006) and references therein, various techniques, mainly based on Monte Carlo simulations, have been successfully utilized for the computation of the so-called probability of instability, and related performance indices. In Marrison and Stengel (1997) robust control system design for a mass–spring–mass system is faced with random search and genetic algorithms, opening to the application of randomization methods for gain synthesis besides robustness analysis. The application area, providing motivations for the development of these methods, was indeed aerospace control.

Since randomized algorithms are an emerging technology in control engineering, to date, contributions in this field have mostly focused on theoretical developments. Hence, in the recent literature it is rarely discussed how the basic technology may be applied to challenging real-world applications. Inevitably, the use of new theoretical results in control requires consideration of issues and incorporation of heuristic techniques that go beyond the theory. The proposed framework herein referring to a small-scale UAV could be, with minor extensions, applicable to other flight control problems. This framework addresses critical application-related issues, such as the computational issues associated with randomized algorithms, the integration of *a priori* domain knowledge, and human designer interaction with automated design.

The paper organization is outlined in the following. Uncertainty description is the focus of Section 2. Uncertainty is represented by the vector $\Delta = [\delta_1 \ \delta_2 \ \cdots \ \delta_\ell]^T$ consisting of ℓ real uncertain random parameters δ_i with an assigned probability density function (p.d.f.), either uniform or Gaussian. Uncertainties for the aerial platform include parameters related to flight conditions, aerodynamic data, geometric and inertial data. In this section, the concept of *specification property* $\mathscr{S}$, which is subsequently utilized in the randomized algorithms, is briefly introduced. In Section 3, three randomized algorithms for gain synthesis and robustness analysis, which should be used sequentially, are presented. The first algorithm is based upon the selection of $m \leqslant \ell$ critical uncertain parameters, and has the objective to provide an initial set of randomly generated controller gains. The so-called "Log-over-log" Bound, see Tempo, Bai, and Dabbene (1997), which requires probabilistic confidence and accuracy, is used as a stopping criterion for the algorithm. A second algorithm uses the set of gains previously obtained and computes the probability (estimated accordingly to the probabilistic approach; see Eq. (10)) that user-defined specifications are satisfied. To this end, a classical bound on the required sample size, the Chernoff Bound is stated. A third algorithm also computes the estimated probability, but different specification properties, derived from standard flying qualities of piloted aircraft, see Anonymous (1997), are used. As an alternative to the randomization-based techniques for gain synthesis (i.e. to the first algorithm described above), a classic pole placement approach is also proposed, see, e.g. Ogata (1995). The gains obtained with this approach are numerically compared with the randomized gains by computing various empirical probabilities. In Section 4 numerical results related to the case study of a reference aerial platform (see Appendix A) are presented. In particular, a plot of the so-called *probability degradation function*, showing how the empirical probability degrades as a function of an "amplification factor" ρ (see this section for a precise definition), is provided. Moreover, the key role of probability degradation for choosing the best gain matrix is discussed in presenting the selection criterion. This section also provides an insight regarding the numerical results for the probabilistic robustness analysis and the simulation results for the time domain response of the aerial platform. Although the design phase is performed using the linearized model of the aircraft, the efficacy of the method is verified by comparing the time response of the complete nonlinear model to the performance specification based on the standard requirements. An extensive discussion regarding the comparisons in terms of stability and performance robustness is reported. The effectiveness of the two proposed approaches (randomized and pole placement) to gain synthesis is also tested. Finally, a brief conclusion is given in Section 5. In Appendix A the aircraft mathematical model, based upon a full six degrees-of-freedom nonlinear model (see Stevens & Lewis, 2003), is outlined. This model was linearized to provide state-space characterization of the uncertain system and it was used in the full nonlinear form to implement numerical simulations. In Appendix B the meta-algorithms are reported, in order to complete and clarify the algorithm description in Section 3.

2. Random uncertainty description and probabilistic bounds

To characterize parametric uncertainty, the linearized system is written using the standard state-space formulation

$$\dot{x}(t) = A(\Delta)x(t) + B(\Delta)u(t), \tag{1}$$

where $A \in \mathbf{R}^{n,n}, B \in \mathbf{R}^{n,p}$ and Δ consists of ℓ real time-invariant uncertain parameters, i.e. $\Delta = [\delta_1 \ \cdots \ \delta_\ell]^T$. The implemented controller structure is a state-feedback of the form $u = -Kx$, so that the problem is to find a gain matrix $K \in \mathbf{R}^{p,n}$ satisfying given specifications.

Next, each uncertain parameter δ_i is assumed to be a random variable distributed according to a given probability density function $p(\delta_i)$. In particular, the parameter δ_i may be uniformly distributed or distributed according to a Gaussian density. That is, for a uniform distribution $\mathscr{U}[\delta_i]$, the p.d.f. can be expressed as

$$p(\delta_i) = \mathscr{U}[\delta_i] = \begin{cases} \dfrac{1}{\delta_i^+ - \delta_i^-} & \text{if } \delta_i \in [\delta_i^-, \delta_i^+], \\ 0 & \text{otherwise.} \end{cases} \tag{2}$$

The normal (Gaussian) distribution $\mathscr{N}[\delta_i]$ with mean $\bar{\delta}_i$ and variance σ^2 is given by

$$p(\delta_i) = \mathscr{N}[\delta_i] = \frac{1}{\sigma\sqrt{2\pi}} \mathrm{e}^{-(1/2)(\delta_i - \bar{\delta}_i)^2/\sigma^2}. \tag{3}$$

For uniform distribution, the support set of the density function $p(\Delta) = \prod_i p(\delta_i)$ is denoted by $\mathscr{B}_\Delta$, whereas, in the case of normal distribution, the support set coincides with $\mathbf{R}^\ell$. Then, N_Δ independent identically distributed (i.i.d.) samples $\Delta^j = [\delta_1^j \ \cdots \ \delta_\ell^j]^T$ of the random vector Δ are considered. In particular, this means that the random sample δ_i^j of the parameter δ_i is drawn according to the distribution $p(\delta_i)$.

The next step is to introduce a *specification property* $\mathscr{S}$ which is the set of all specifications to be satisfied by the closed-loop system $\dot{x} = (A - BK)x$. In particular, $\mathscr{S}_{RGS}$ refers to controller synthesis, while $\mathscr{S}_{RSRA}$ and $\mathscr{S}_{RPRA}$ are related to stability and performance robustness, respectively. Concrete instances of specification properties for the aerial platform are provided in Section 4 and include, for example, limits on the step or frequency response, or restrictions of natural frequency and damping ratio within a given range.

In the probabilistic design phase, the gain matrix K is assumed to be random too. Then, N_K i.i.d. matrix samples $\{K^1, K^2, \ldots, K^{N_K}\}$ are considered. In particular, the sample k_{im}^j of the random gain k_{im} is drawn within the given interval $[k_{im}^-, k_{im}^+]$ according to a uniform distribution. The range of variation for controller gains is guessed according to the closed loop referred to the nominal system and to the designer's knowledge of platform dynamics. The set $\mathscr{B}_K$ is defined as

$$\mathscr{B}_K = \{K : k_{im} \in [k_{im}^-, k_{im}^+], i = 1, 2, \ldots, p, m = 1, 2, \ldots, n\}. \tag{4}$$

The objective is to find a gain matrix $K_{rand} = K^j$ which satisfies the specification property $\mathscr{S}_{RGS}$.

Clearly, it is important to determine the sample size N_K which provides a stopping rule in the randomized algorithms described later in Section 3. To this end, an explicit bound, often denoted as "Log-over-log," is provided (see Eq. (7)). It is based on two probabilistic quantities, restricted within the intervals $(0, 1)$, denoted as accuracy ε and confidence η. This bound has been introduced in Tempo et al. (1997), see also Fujisaki, Oishi, and Tempo (2008). Before stating this bound, the volume of the set, denoted as the *good set*, of all controller gains satisfying the specification property $\mathscr{S}_{RGS}$ is defined as

$$\mathrm{Vol}_{good} = \mathrm{Vol}\{K \in \mathscr{B}_K : \mathscr{S}_{RGS} \text{ is satisfied}\}. \tag{5}$$

On the other hand, the volume of the set $\mathscr{B}_K$ is expressed as

$$\mathrm{Vol}_{\mathscr{B}_K} = \prod_{i=1}^{p}\prod_{m=1}^{n}(k_{im}^+ - k_{im}^-). \tag{6}$$

2.1. Log-over-log Bound

For any accuracy $\varepsilon \in (0, 1)$ and confidence $\eta \in (0, 1)$, let

$$N_K \geqslant \frac{\log(1/\eta)}{\log(1/(1-\varepsilon))}. \tag{7}$$

Then, if $\mathrm{Vol}_{good} > \varepsilon \mathrm{Vol}_{\mathscr{B}_K}$, the probability that there is no K^j, $j = 1, 2, \ldots, N_K$, in $\mathscr{B}_K$ satisfying $\mathscr{S}_{RGS}$ is less than η.

A graphical interpretation of these concepts is given in Tempo et al. (2005).

Let $\{K^1, K^2, \ldots, K^s\}$ be the random matrices satisfying $\mathscr{S}_{RGS}$, where s denotes the number of *successes*, i.e. the number of matrix gains satisfying $\mathscr{S}_{RGS}$. The second (robustness) phase utilizes $K_{rand} = K^j$, $j = 1, 2, \ldots, s$, previously computed and has the objective to estimate the "true" probability p_{true} that the specification property $\mathscr{S}_{RSRA}$ is satisfied. That is, formally

$$p_{true} = \mathrm{Prob}\{\Delta \in \mathscr{B}_\Delta : \mathscr{S}_{RSRA} \text{ is satisfied}\}. \tag{8}$$

Then, the indicator function is defined as follows:

$$\mathscr{I}(\Delta^j) = \begin{cases} 1 & \text{if } \Delta^j \text{ satisfies } \mathscr{S}_{RSRA}, \\ 0 & \text{otherwise.} \end{cases} \tag{9}$$

Although ideally preferable, the exact computation of the probability p_{true} requires to solve a multiple integral with a domain which is hard to describe explicitly. For this reason, resorting to randomization, a probabilistic approximation of p_{true} is computed. Due to the finite sample size, the estimated probability that the specification property $\mathscr{S}_{RSRA}$ is satisfied is immediately given by

$$\widehat{p}_{N_\Delta} = \frac{1}{N_\Delta}\sum_{j=1}^{N_\Delta}\mathscr{I}(\Delta^j). \tag{10}$$

The estimate $\widehat{p}_{N_\Delta}$ is usually referred to as the *empirical probability*. Clearly, it is important to determine the sample size N_Δ to obtain a reliable probabilistic estimate $\widehat{p}_{N_\Delta}$. To this purpose, the Chernoff Bound can be used, see Chernoff (1952).

2.2. Chernoff Bound

For any accuracy $\varepsilon \in (0, 1)$ and confidence $\eta \in (0, 1)$, let

$$N_\Delta \geqslant \frac{1}{2\varepsilon^2}\log\left(\frac{2}{\eta}\right). \tag{11}$$

Then, the probability that $|\widehat{p}_{N_\Delta} - p_{true}| > \varepsilon$ holds is less than η.

It is important to remark that the sample size given by the Log-over-log and Chernoff bounds does not depend on the number of uncertain parameters and on the probability distribution $p(\Delta)$. Hence, these bounds are problem independent and explicit so that an *a priori* computation could be performed. This is in contrast to classical confidence intervals, see, e.g. Ray and Stengel (1993), which require standard tables which are based on the outcome of the sample generation process, i.e. on the specific realization of the random samples. Clearly, an important issue is the development of efficient algorithms for sample generation according to various distributions. Further discussions on this topic can be found in Tempo et al. (2005).

Furthermore, it is noteworthy that Chernoff-like bounds hold if the samples Δ^j are i.i.d. If this assumption does not hold, different randomization schemes based on Markov chains may be considered. For example, the well-known hit-and-run method (see, e.g. Tempo et al., 2005) for generating random samples within convex sets may be used.

3. Randomized algorithms and robustness analysis

As previously discussed, the controller structure is a state-feedback of the form $u = -Kx$, so that the control problem is to find a suitable gain matrix K. By considering this controller structure, the assumption that the states are available all the time is made. For this reason the design does not include the observer structure. In this section, randomized and deterministic algorithms are presented for gain synthesis, stability and performance analysis. The algorithms are closely related to the operating flight conditions and to the flying quality standards. In particular, Algorithm RGS (randomized) or Algorithm PP (deterministic) are used for providing an initial set of controller gains, while Algorithm RSRA and Algorithm RPRA have the objective to check (probabilistic) robustness of those gains. The performance requirements specified in Algorithm RPRA may be different than those of Algorithm RSRA, so that refinements on the choice of gains may be obtained by applying a selection metric, aimed at identifying the best trade-off (see Section 4). The proposed algorithms are herein outlined. Detailed meta-algorithms are given in Appendix B.

Algorithm RGS is based upon the selection of $m \leqslant \ell$ *critical* uncertain parameters. That is, a vector $\Delta_c = [\delta_1 \ \delta_2 \ \cdots \ \delta_m]^T$, containing only $m \leqslant \ell$ components of the vector of uncertain parameters, is considered. The selection of a potentially reduced number of critical uncertain parameters allows to reduce computational workload in the design phase. Selection criteria are based on designer's experience and knowledge of the specific application. The critical uncertain parameters are set to all combinations of their upper or lower values[1] δ_i^+ or δ_i^- and the remaining non-critical parameters are set to their corresponding nominal value, i.e. $\delta_i^0, i = m+1, \ldots, \ell$. Clearly, since the state-space matrix $A(\Delta)$ depend on Δ, this requires to compute $M = 2^m$

[1] In the case of Gaussian-distributed parameters, the upper and lower bounds may be chosen as $\delta_i^\pm = \bar{\delta}_i \pm 3\sigma_i$, where $\bar{\delta}_i$ is the nominal value of the i-th uncertain parameter.

Table 1
Computational workload for the proposed algorithms ($m = 2$, $N_K = 200,000$, $s = 5$, $N_\Delta = 5000$).

Algorithm	Sample gen.	Synthesis	Analysis	Other	Total
RGS	$0.005T$	$0.994T$	–	$0.001T$	T
PP	–	$0.0001T$	–	$0.004T$	$0.0041T$
RSRA	$6.91T$	–	$0.027T$	$0.003T$	$6.94T$
RPRA	$6.91T$	–	$0.08T$	$0.01T$	$7T$

T is reference machine time.

critical matrices of the form

$$A_c^1 = A(\delta_1^+, \delta_2^+, \ldots, \delta_m^+, \delta_{m+1}^0, \ldots, \delta_\ell^0), \tag{12}$$

$$A_c^2 = A(\delta_1^-, \delta_2^+, \ldots, \delta_m^+, \delta_{m+1}^0, \ldots, \delta_\ell^0), \tag{13}$$

$$\vdots \tag{14}$$

$$A_c^M = A(\delta_1^-, \delta_2^-, \ldots, \delta_m^-, \delta_{m+1}^0, \ldots, \delta_\ell^0). \tag{15}$$

The critical matrices B_c^i, $i = 1, \ldots, M$, are computed accordingly for the input matrix $B(\Delta)$. It can be observed that the computational complexity increases exponentially as the number of critical parameters increases. Next, taking a uniform p.d.f. for the controller gain parameters, Algorithm RGS verifies the fulfillment of a specification property $\mathscr{S}_{RGS}$. It should be remarked that the algorithm terminates after a number of iterations dictated by the Log-over-log Bound thus providing a set of gains $\{K^1, K^2, \ldots, K^s\}$ such that $A_{cl}(K^i) = A_c - B_c K^i$ satisfies $\mathscr{S}_{RGS}$.

If $s = 0$ is obtained, the gain matrix provided by a classical pole placement technique, see, e.g. Ogata (1995), may be considered for the subsequent robustness analysis phases. The resulting algorithm is denoted as *Algorithm PP*, which is presented for the single-input case. The user-defined requirements are specified in terms of desired pole locations, with reference to the nominal flight condition.

The starting point of *Algorithm RSRA* is the use of the gains previously obtained and the specification property $\mathscr{S}_{RSRA}$. For each gain matrix $\overline{K}$ provided either by Algorithm RGS or by Algorithm PP, this algorithm is based on randomization of all uncertain parameters (and not only the critical ones), according to a specified distribution $p(\Delta)$. Given accuracy $\varepsilon \in (0, 1)$ and confidence $\eta \in (0, 1)$, the Chernoff Bound is used for computing the required sample size. The empirical probability of

$$\text{Prob}\{\Delta \in \mathscr{B}_\Delta : A_{cl}(\Delta) = A(\Delta) - B(\Delta)\overline{K} \text{ satisfies } \mathscr{S}_{RSRA}\} \tag{16}$$

is computed.

Algorithm RPRA is finally utilized. This algorithm has a structure similar to Algorithm RSRA, but a different specification property $\mathscr{S}_{RPRA}$, based on performance metrics referred to flying and handling qualities (see Anonymous, 1997), is introduced. The corresponding empirical probability of

$$\text{Prob}\{\Delta \in \mathscr{B}_\Delta : A_{cl}(\Delta) = A(\Delta) - B(\Delta)\overline{K} \text{ satisfies } \mathscr{S}_{RPRA}\} \tag{17}$$

is computed using the same sample size obtained in Algorithm RSRA.

A comparison of computational complexity of the proposed algorithms is provided in Table 1, with reference to the practical case study discussed in Section 4.[2] As a matter of fact, stability and performance analysis involve an higher workload than the gain synthesis phase. It is noteworthy that the high computational time for Algorithm RSRA and Algorithm RPRA is mainly related to the generation of random matrices of uncertain parameters. Therefore the computational complexity is directly affected by accuracy and confidence parameters through the sample size N_Δ (see Eq. (11)). Whereas an increase in the degree of confidence η is demonstrated to be feasible, the accuracy ε strongly influences the computational complexity. As a matter of fact, an increase of two orders of magnitude for the confidence η requires to approximately double the sample size. On the other hand, for a degree of confidence $\eta = 0.001$, reducing the accuracy parameter ε from 0.02 to 0.01 entails a redoubling of the sample size.

[2] As to the current implementation on a 2.5 GHz computer platform, the reference machine time T reported in Table 1 is roughly 30 min.

4. Control design for the MH1000 platform

The proposed methodology has been applied to the design of an embedded real-time system for autonomous flight control of the MH1000 platform (see Appendix A). The numerical experiments reported here are based on the assumption of decoupled dynamics and deal with the longitudinal plane dynamics stabilization. In particular, attention is focused on a full state feedback longitudinal control of the form $u = -Kx = \eta_e$, just controlled by the symmetrical elevon deflection η_e. The state vector $x \in \mathbf{R}^4$ is defined as $x = [V\ \alpha\ q\ \theta]^T$, where V is the flight speed, α is the angle of attack, q is the pitch rate and θ is the pitch angle. State and control matrices characterizing the nominal reference condition ($V = 43$ ft/s and $h = 164$ ft) are obtained by numerical linearization

$$A = \begin{bmatrix} -0.293 & -0.486 & -0.0002 & -9.812 \\ -0.113 & -6.181 & 0.914 & -0.0003 \\ 0.000 & -64.83 & -8.074 & 0.000 \\ 0.000 & 0.000 & 1.000 & 0.000 \end{bmatrix}, \quad B = \begin{bmatrix} -0.7914 \\ -3.9250 \\ -443.487 \\ 0.000 \end{bmatrix}. \tag{18}$$

Next, it should be noted that structured parameter uncertainties are taken into account, including those related to flight conditions (dynamic pressure), aerodynamic data (stability and control derivatives), geometric and inertial data. Uncertainties related to the flight conditions can be ascribed to the real flight in a non-ideally calm air and to the need to cover a portion of the flight envelope as large as possible. Uncertainties concerning the aerodynamic data can be related to experimental measurement errors or computational approximations due to round-off errors. Uncertainties in terms of geometric and inertial data may take into account manufacturing inaccuracies. Moreover, classical references on probabilistic robustness analysis (see, e.g. Ray & Stengel, 1992) deal with uncertain parameters such as wing surface, wing aerodynamic chord, mass and moments of inertia. The real time-invariant parametric uncertainties $\Delta \in \mathbf{R}^{16}$ are described in Tables 2 and 3. Although these uncertainties are partially coupled through the aerodynamic database, they are treated as independent so that the random samples Δ^j are i.i.d. For simplicity, in these tables only approximate values of upper and lower bounds are shown.

In the remainder, the numerical results, obtained with the algorithms described in Section 3, are presented.

Table 2
Plant and flight condition uncertainties definition.

No.	Parameter	p.d.f.	δ_i	%	δ_i^-	δ_i^+
1	Flight speed (ft/s)	$\mathscr{U}$	42.65	±15	36.25	49.05
2	Altitude (ft)	$\mathscr{U}$	164.04	±100	0.00	328.08
3	Mass (lb)	$\mathscr{U}$	3.31	±10	2.98	3.64
4	Wingspan (ft)	$\mathscr{U}$	3.28	±5	3.12	3.44
5	Mean aero chord (ft)	$\mathscr{U}$	1.75	±5	1.67	1.85
6	Wing surface (ft^2)	$\mathscr{U}$	5.61	±10	5.06	6.18
7	Moment of inertia (lb ft^2)	$\mathscr{U}$	1.34	±10	1.21	1.48

Table 3
Aerodynamic database uncertainties definition.

No.	Parameter	p.d.f.	$\bar{\delta}_i$	σ_i
8	C_X coefficient (–)	$\mathcal{N}$	−0.01215	0.00040
9	C_Z coefficient (–)	$\mathcal{N}$	−0.30651	0.00500
10	C_m coefficient (–)	$\mathcal{N}$	−0.02401	0.00040
11	C_{X_q} coefficient (rad^{-1})	$\mathcal{N}$	−0.20435	0.00650
12	C_{Z_q} coefficient (rad^{-1})	$\mathcal{N}$	−1.49462	0.05000
13	C_{m_q} coefficient (rad^{-1})	$\mathcal{N}$	−0.76882	0.01000
14	C_{X_δ} coefficient (rad^{-1})	$\mathcal{N}$	−0.17072	0.00540
15	C_{Z_δ} coefficient (rad^{-1})	$\mathcal{N}$	−1.41136	0.02200
16	C_{m_δ} coefficient (rad^{-1})	$\mathcal{N}$	−0.94853	0.01500

4.1. Gain synthesis

4.1.1. Random gain synthesis—Algorithm RGS

In the following, flight speed and mass are selected as critical uncertain parameters for the gain synthesis phase, i.e. the vector Δ_c is given by $\Delta_c = [\delta_1, \delta_3]^T$. The flight speed has been chosen as critical parameter in order to optimize robustness to environmental changes (due to external disturbances or changes in operating conditions), while the take-off mass represents a key parameter in mission profile definition and flight performance evaluation. In fact, the payload weight fraction may change depending on the airborne systems specifically needed for performing a mission task. The lower and upper bounds of the critical uncertain parameters are reported in Table 2.

The closed-loop specification property $\mathscr{S}_{RGS}$ is defined as follows:

$$\begin{cases} \omega_{SP} \in [4.0, 6.0]\,\text{rad/s}; \quad \zeta_{SP} \in [0.5, 0.9], \\ \omega_{PH} \in [1.0, 1.5]\,\text{rad/s}; \quad \zeta_{PH} \in [0.1, 0.3], \\ \Delta\omega_{SP} = \omega_{upper} - \omega_{lower} < \pm 45\%, \\ \Delta\omega_{PH} = \omega_{upper} - \omega_{lower} < \pm 20\%, \end{cases} \tag{19}$$

where ω and ζ are the undamped natural frequency and the damping ratio of the system characteristic modes, respectively. The subscripts *SP* and *PH* refer to the short period and the phugoid mode, characterizing the aircraft motion in the longitudinal plane. The specification property definition is strictly related to the user needs in terms of mission profile and to the reference platform dynamics. From the properties specified above, it can be observed that completely decoupled dynamics with classical modal characterization (two periodic stable modes) are required for the MH1000 platform. It has to be noted that the closed-loop properties of $\mathscr{S}_{RGS}$ define desired pole location regions in the complex plane.

The number of random samples for the K matrix, computed according to the Log-over-log Bound with $\varepsilon = 4 \times 10^{-5}$ and $\eta = 3 \times 10^{-4}$, is $N_K = 200,000$. The number of successes found through Algorithm RGS, i.e. the number of random gain matrices K^j, $j = 1, 2, \ldots, s$, satisfying the specification property $\mathscr{S}_{RGS}$ is $s = 5$ (see Table 4).

4.1.2. Pole placement—Algorithm PP

A classical pole placement technique has been applied to the MH1000 platform by specifying the desired dynamic characteristics (in terms of natural frequency and damping ratio of the two characteristic modes) and then defining the desired pole locations. The desired dynamics is specified as follows:

$$\begin{cases} \omega_{SP}^{des} = 5.0\,\text{rad/s}; \quad \zeta_{SP}^{des} = 0.7, \\ \omega_{PH}^{des} = 1.25\,\text{rad/s}; \quad \zeta_{PH}^{des} = 0.2, \end{cases} \tag{20}$$

Table 4
Set of gains obtained from gain synthesis phase.

Gain	K_V	K_α	K_q	K_θ
K^1	0.00044023	0.09465000	0.01577400	−0.00473510
K^2	0.00021450	0.09581200	0.01555500	−0.00323510
K^3	0.00054999	0.09430800	0.01548200	−0.00486340
K^4	0.00010855	0.09183200	0.01530000	−0.00404380
K^5	0.00039238	0.09482700	0.01609300	−0.00417340
K^{PP}	0.00057038	0.09643700	0.01379500	−0.00458900

where symbols and subscripts have the meaning previously specified for the RGS algorithm and *des* indicates "desired."

The gain matrix K^{PP}, obtained by applying the pole placement technique to the nominal model, is reported in Table 4.

4.2. Probabilistic robustness analysis

4.2.1. Stability robustness analysis—Algorithm RSRA

The uncertain parameters considered in this phase, their nominal values, probability density function and tolerances are given in Tables 2 and 3. As it can be observed, uniform ($\mathscr{U}$) and Gaussian ($\mathscr{N}$) probability density functions have been used to characterize parameter uncertainties: geometric, inertial and operational uncertainties are characterized by uniform p.d.f. while the uncertainties related to the aerodynamic database are characterized by a Gaussian probability density function. This criterion has been adopted due to the nature of the parameters: the value of the aerodynamic derivative should have higher probability close to the nominal value experimentally or numerically obtained.

For this specific application, the specification property $\mathscr{S}_{RSRA}$ coincides with $\mathscr{S}_{RGS}$ (see Eq. (19)). The number of samples for the specification property $\mathscr{S}_{RSRA}$ is obtained by the Chernoff Bound with $\varepsilon = 0.0145$ and $\eta = 0.0145$ and is equal to $N_\Delta = 5000$.

Next, the so-called *probability degradation function* is described. This function has the objective to evaluate the amount of uncertainty that can be tolerated by plant and flight condition uncertainties, when there is no uncertainty affecting the aerodynamic database. More precisely, the aerodynamic database uncertain parameters, δ_i, $i = 8, 9, \ldots, 16$, are equal to their nominal values $\bar{\delta}_i$, $i = 8, 9, \ldots, 16$. The plant and flight condition uncertainty intervals $[\delta_i^-, \delta_i^+], i = 1, 2, \ldots, 7$ are multiplied by the "amplification factor" $\rho > 0$. That is

$$\delta_i \in \rho[\delta_i^-, \delta_i^+], \quad i = 1, 2, \ldots, 7. \tag{21}$$

The result is that the width of the interval is multiplied by ρ, but the center of the interval (nominal value) is unchanged. The empirical probability of stability is then computed using Algorithm RSRA for several values of ρ in the interval $[0, 1.5]$. The resulting probability degradation function is shown in Fig. 1. This plot highlights great differences in controller gains behavior, in terms of both individual value and rate of variation. Increasing the amplification factor from $\rho_1 = 0.75$ to $\rho_2 = 1.25$, a doubling of the difference between the upper and the lower probability degradation curve (referring to K^4 and K^5, respectively) can be observed.

4.2.2. Performance robustness analysis—Algorithm RPRA

The methodology utilized in this phase is very similar to that applied for stability robustness. In particular, the uncertain parameters, the sample size $N_\Delta = 5000$, the random samples Δ^j

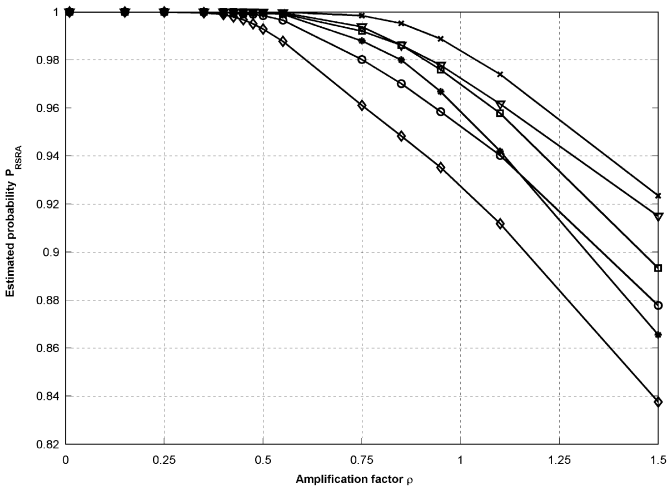

Fig. 1. Probability degradation function obtained with Algorithm RSRA (K^1—circle; K^2—asterisk; K^3—square; K^4—cross; K^5—diamond; K^{PP}—triangle).

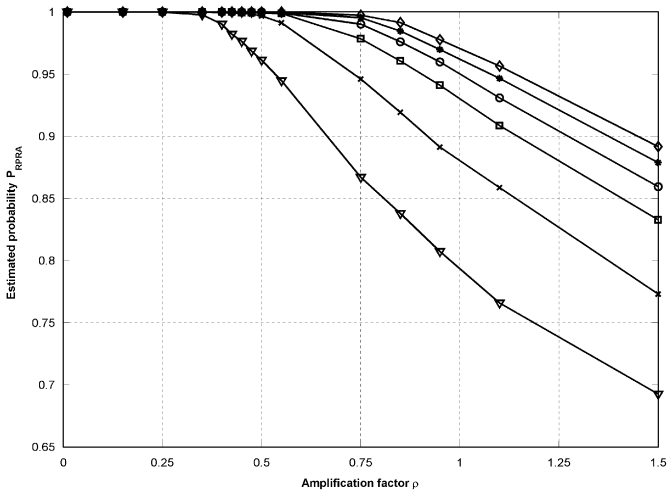

Fig. 2. Probability degradation function obtained with Algorithm RPRA (K^1—circle; K^2—asterisk; K^3—square; K^4—cross; K^5—diamond; K^{PP}—triangle).

and the gains $\overline{K}$ coincide with those of Algorithm RSRA. The specification property $\mathscr{S}_{RPRA}$ is referred to levels and qualitative "suitability" of flying qualities, see Anonymous (1997). Level 1, corresponding to a satisfactory degree of "suitability," is considered to define target closed-loop properties. A frequency response criterion, involving the bandwidth ω_{BW} and the phase delay τ_P of the actual higher-order system, has been selected.[3]

The specification property $\mathscr{S}_{RPRA}$ is defined in order to meet the requirements in terms of short-term pitch response as

$$\begin{cases} \omega_{BW} \in [2.5, 5.0]\,\text{rad/s}, \\ \tau_P \in [0.0, 0.05]\,\text{s}. \end{cases} \tag{22}$$

It has to be noted that the closed-loop properties of $\mathscr{S}_{RPRA}$ identify specific regions of interest in the $\omega_{BW}-\tau_P$ plane.

In this case, the empirical probability of performance is computed using Algorithm RPRA. The resulting probability degradation function, reported in Fig. 2, provides conclusions on controller behavior similar to those concerning stability robustness. In some cases (see, e.g. K_{PP}) markedly lower estimated probabilities and worse degradation trend can be noticed.

4.3. Best gain selection

Numerical results of the empirical probabilities of fulfilling stability and performance requirements for different gains, for a nominal value of amplification factor $\rho = 1$, are reported in Table 5.

Graphical tools as well as numerical methods have been utilized to perform robustness analysis of the designed closed-loop system. As to stability robustness, probabilistic root locus has been used to characterize different gain sets in terms of probability to fulfill the specification property $\mathscr{S}_{RSRA}$. Fig. 3, reporting a comparison between the root locus plot for controllers K^2 and K^4, clearly picks out that K^2 could give rise to some unstable conditions when all uncertain parameters are considered. Therefore, K^2 should be discarded from the set of satisfactory solutions, despite the estimated probability values numerically computed. It is noteworthy that the four sectors identified by solid lines represent the desired pole location regions, as defined by the closed-loop properties of $\mathscr{S}_{RSRA}$.

Table 5
Empirical probabilities for stability and performance robustness, and results of the selection criterion.

Gain	P^i_{RSRA} (%)	P^i_{RPRA} (%)	P^i_W (%)	ΔP^i_W	P^i_{TOT}
K^1	88.56	93.58	90.07	8.2405	9.1411
K^2	90.60	95.16	91.97	7.6971	8.6167
K^3	89.31	90.80	89.76	8.6741	9.5717
K^4	93.86	84.78	91.14	10.8689	11.7802
K^5	85.14	96.06	88.42	7.8277	8.7119
K^{PP}	96.27	76.06	90.21	9.3415	10.2436

Comparing the controller gains resulting from randomized approach (Algorithm RGS) to that obtained through a classical pole placement (Algorithm PP), it can be noted that good stability robustness characteristics can be obtained using the latter method. As a matter of fact, the desired dynamics defined by the user can properly fit the stability metrics of specification property $\mathscr{S}_{RSRA}$. On the other hand, the estimated probability shown by the K^{PP} in terms of performance metrics is extremely poor (see Fig. 4). However, it is noteworthy that pole placement is designed for stability purposes and it is not intended to fulfill performance requirements. On the other hand, conventional control design techniques such as μ-synthesis would provide satisfactory stability and performance specifics, but entail the implementation of high-order controllers.

Several criteria could be implemented for selecting the best solution according to stability and performance robustness. For the present application, the selection is based on a trade-off between the probability features for a specific amount of uncertainty and their trend as the uncertainty increases. As a matter of fact, the criterion adopted to select the best solution K^* can be formulated as follows:

$$K^* = \arg\max_{K^i \in \mathscr{K}} \{[w_1 P^i_{RSRA} + w_2 P^i_{RPRA}] + [\tilde{w}_1 \Delta P^i_{RSRA} + \tilde{w}_2 \Delta P^i_{RPRA}]\}, \tag{23}$$

where $\mathscr{K} = \{K^1, K^2, \ldots, K^5\}$, $w_1 = 0.7$, $w_2 = 0.3$, $\tilde{w}_1 = 0.07$, $\tilde{w}_2 = 0.03$, and P_{RSRA} and P_{RPRA} are the empirical probabilities of

[3] It has to be noted that the "bandwidth," as defined for handling quality criterion purposes in Anonymous (1997), is the highest frequency at which the phase margin is at least 45° and the gain margin is at least 6 dB.

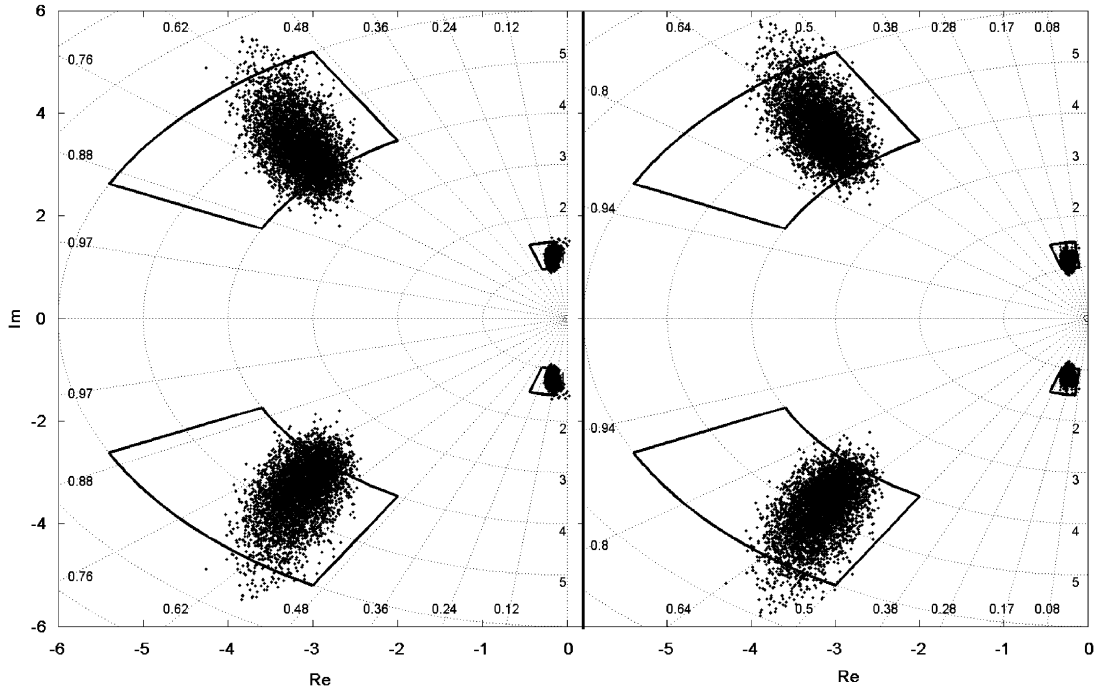

Fig. 3. Root locus plot for K^2 (left) and K^4 (right) highlighting the regions of interest for stability robustness analysis.

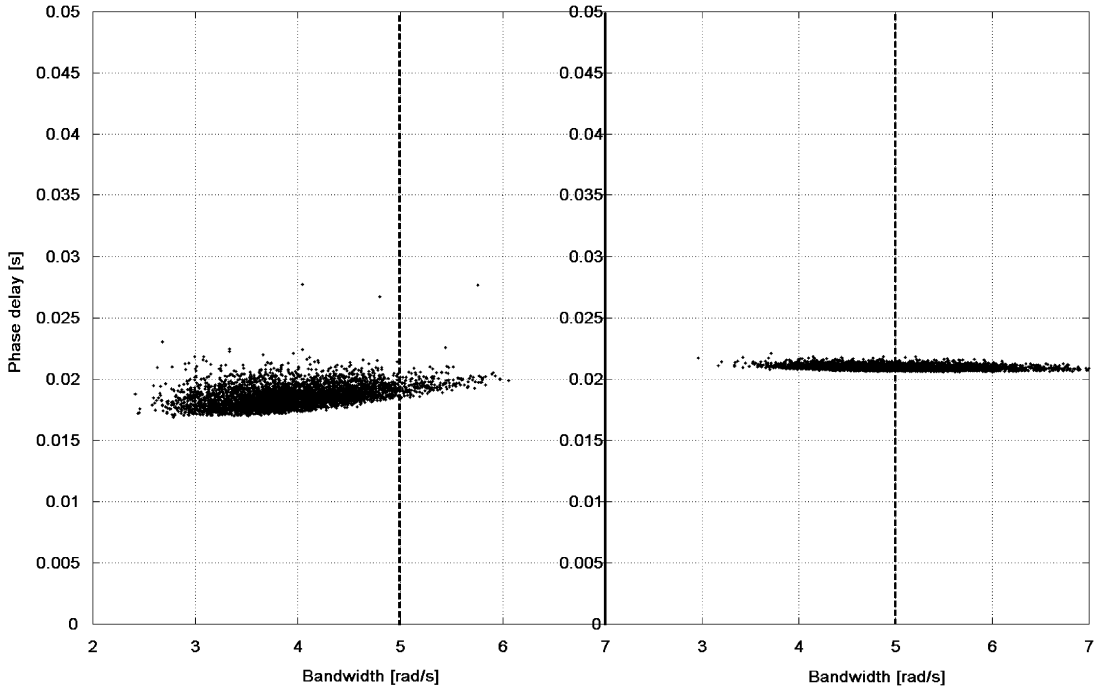

Fig. 4. Bandwidth criterion plot for K^5 (left) and K^{PP} (right) highlighting the regions of interest for performance robustness analysis.

satisfying $\mathscr{S}_{RSRA}$ and $\mathscr{S}_{RPRA}$, respectively; their values for the gain sets under consideration are shown in Table 5. It can be noticed that w_1, w_2, $\tilde{w}_1$ and $\tilde{w}_2$ are user-defined weights, selected according to the controller design requirements and the user experience of the platform dynamics. Furthermore

$$\Delta P^i_{RSRA} = \left| \frac{\rho_2 - \rho_1}{P^i_{RSRA}(\rho_2) - P^i_{RSRA}(\rho_1)} \right|, \tag{24}$$

where $\rho_1 = 0.75$, $\rho_2 = 1.25$, and values of $P^i_{RSRA}(\rho_1)$ and $P^i_{RSRA}(\rho_2)$ can be determined from the probability degradation function. ΔP^i_{RPRA} is defined accordingly. Eq. (23) can be rewritten as

$$K^* = \arg\max_{K^i} \{P^i_W + \Delta P^i_W\}, \tag{25}$$

where P^i_W represents a weighted probability and ΔP^i_W represents a measure of the probability degradation as a function of the uncertainty amplification factor ρ. Results of the application of this selection criterion to the present case study are reported in Table 5. It should be noted that, while P^i_W (fourth column) represents a probability, ΔP^i_W and P^i_{TOT} (fifth and sixth column, respectively) do have not the same meaning.

Finally, as shown by numerical values, the RGS algorithm is able to guarantee weighted probability of stability higher than the pole placement technique. In particular, according to the above reported selection criterion, the gain matrix K^4 is chosen as the best fit which satisfies a good compromise between stability and performance requirements, in terms of individual values and probability degradation features.

4.4. Time domain response simulations

The time domain responses of the linearized system as well as of the complete nonlinear system (see Appendix A), have been analyzed in the closed-loop configuration, by implementing the gain matrices resulting from the randomized and classical synthesis. It should be noted that the gain synthesis techniques are based on the state-space formulation of the aircraft dynamics and, hence, on the linearized system. Therefore, the full nonlinear model represents a invaluable tool to test the controller effectiveness.

Deterministic time responses have been obtained through the nonlinear model by referring to the nominal operating condition ($V = 43$ ft/s; $h = 164$ ft), whereas stochastic time responses have been obtained by applying the linearized model to the uncertain systems.

Deterministic simulation results allow to evaluate and compare closed-loop system performance with reference to the time domain. As an example, Fig. 5 shows the time domain responses related to the gain sets of Table 4, referring to a flight speed command. The command response envelope, whose bounds can be defined according to standard criteria, see Anonymous (1997), gives an estimation of "goodness" of time responses. It can be observed that all the closed-loop systems violate the step bounds as to peak overshoot. The better response, in terms of overshoot, settling time and steady state error, is given by the controller gain K^4, whose deviation from the envelope bounds is less than 5% of the command magnitude.

Fig. 6 shows randomized time responses for the controller gain K^4 to an angle-of-attack command according to the linearized model. Deviations from the command response envelope can be observed, mainly concerning peak overshoot and steady state error. It is noteworthy that a considerable improvement of controller performance as to time domain response may be obtained by including the step bounds in the specification property $\mathscr{S}_{RGS}$.

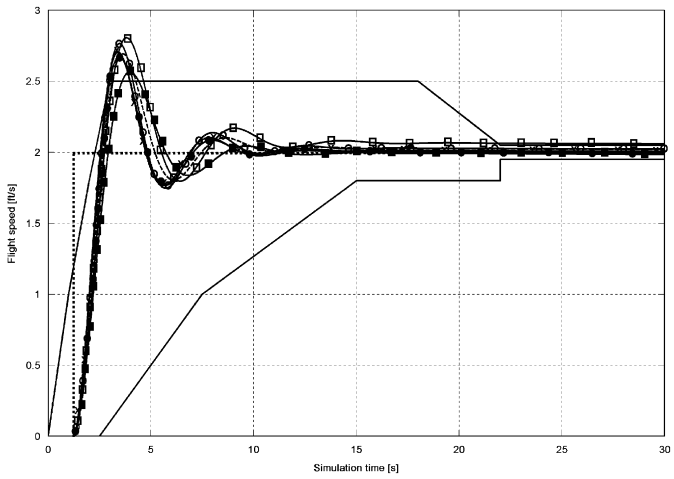

Fig. 5. Time domain response: flight speed command (black—reference; filled circle—K^1; empty square—K^2; cross—K^3; filled square—K^4; empty circle—K^5; dashed black—K^{PP}).

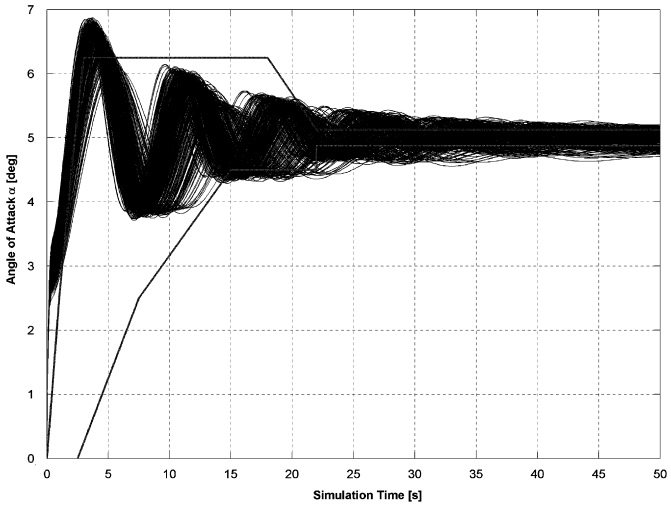

Fig. 6. Time domain response: angle-of-attack command (for $N_\Delta = 500$ uncertain systems).

5. Conclusion

In this paper, a methodology based on the theory of randomized algorithms is presented for gain synthesis and robustness analysis. Results of the application to a Mini-UAV platform are discussed. The proposed methodology demonstrates its effectiveness in dealing with real parametric uncertainties characterized by different probability distributions. A randomized approach to controller synthesis is enforced by taking into account the effects of critical parameters on closed-loop system response to stability and performance metrics. The computational complexity of search and analysis is based on *a priori* bounds, which depend only on accuracy and confidence values. Sample generation and uncertainty dimension are responsible for the high computational workload required by the robustness analysis phase. Numerical results related to the Mini-UAV control design prove the capabilities of the proposed approach in finding a solution able to meet specific user-defined requirements. Although designed according to a linearized model of the aerial platform, the resulting controller demonstrates to satisfactorily perform also with respect to the full nonlinear system.

Acknowledgments

The results presented in this paper are obtained within the Italian National Project Cofin (prot. 2004095094), supported by the Ministry for University and Research. The aerial platform MH1000 is based on the MicroHawk configuration, developed at the Aerospace Engineering Department, Politecnico di Torino (national Patent no. TO2003A000702, holder Politecnico di Torino).

Appendix A. Mathematical model of the aerial platform

The reference aerial platform is a small autonomous aerial vehicle, named MH1000, characterized by 3.28 ft wingspan and a total take-off weight of approximately 3.3 lb. It is based on a conventional layout, characterized by a fixed wing, tailless integrated wing-body, tractor propeller driven. The aerial platform is able to fly at speeds ranging from 33 to 66 ft/s and at a maximum operating altitude of 328 ft. Experimental on-site tests demonstrated that a 40 min flight can be achieved at an average

speed of about 43 ft/s (Pralio, Guglieri, & Quagliotti, 2003; Sanna & Pralio, 2005). The aerial platform, aimed at performing environmental monitoring for fire detection and monitoring, industrial areas reconnaissance and natural disaster monitoring, was developed within national and regional co-funded projects. It was equipped with onboard sensors and cameras to detect environmental conditions and to gather images of the target area. The aerial platform was designed and developed to perform remotely piloted flight as well as autonomous flight, depending on mission profile and user needs. The platform performance and the compliance to project requirements were tested by analytical and real-time simulations of mission profiles. Trajectory optimization, dynamic response analysis, controller architecture design and control synthesis were carried out by modeling the aircraft dynamics and the surrounding environment conditions.

The aerial platform dynamics has been described by a full six degrees-of-freedom nonlinear mathematical model, consisting of twelve, coupled nonlinear, ordinary differential equations, see, e.g. Stevens and Lewis (2003). The model is based on three translational equations, three attitude dynamics equations, three kinematical relationships, and three navigation equations for trajectory evaluation. Classical assumptions of rigid body and flat and non-rotating Earth are made. These assumptions are supported by the application to a Mini-UAV, characterized by small dimensions and weight, performing low speed flight over a small region of the Earth, see Etkin (2003).

The equations of motion are given with reference to the wind–axes reference frame, i.e. a system having origin at the vehicle center of gravity and axes aligned to the flight trajectory. The nonlinear model is expressed in terms of the state variables

$$X^T = [V\ \ \beta\ \ \alpha\ \ P_S\ \ Q\ \ R_S\ \ \phi\ \ \theta\ \ \psi\ \ X_V\ \ Y_V\ \ Z_V]. \tag{A.1}$$

Four blocks of three state variables could be identified. The first three state variables are flight speed, angle of attack and sideslip angle, respectively, the next three variables are the stability–axes components of the angular velocity vector, the third block consists of Euler angles describing aircraft attitudes, and the last block contains the aircraft position coordinates with respect to the local navigation reference system.

The 12 equations are herein reported in matrix notation. The translational equations are formulated with reference to the wind–axes reference frame

$$\{\dot{V}_E\}_W + [\Omega_{\omega_{W/B}}]_W\{V_E\}_W = \frac{1}{m}\{F_{A,T}\}_W - [\Omega_{\omega_W}]_W\{V_E\}_W - [T_{VW}]^{-1}\{g\}_V, \tag{A.2}$$

where $\{V_E\}_W = [V\ \ 0\ \ 0]^T$ is the linear velocity vector, m is the aircraft mass, $\{F_{A,T}\}_W$ are the aerodynamic and propulsive forces, respectively, and $\{g\}_V = [0\ \ 0\ \ g]^T$ is the gravity acceleration vector with reference to the local navigation system. The matrix T_{VW} represents the rotation matrix from wind to local navigation reference system. The terms $[\Omega_{\omega_{W/B}}]_W$ and $[\Omega_{\omega_W}]_W$ represent the cross-product matrices of the angular velocity vector between wind and body axes $\{\omega_{W/B}\} = [-\dot{\alpha}\sin\beta\ \ -\dot{\alpha}\cos\beta\ \ -\dot{\beta}]^T$ and the angular velocity vector of the wind reference frame $\{\omega_W\}$, respectively. It has to be noted that the left-hand side of Eq. (A.2) contains the derivatives of the first three state variables (see Eq. (A.1)).

The rotational dynamics is described by the following equations:

$$\{\dot{\omega}\}_S = -[\Omega_{\omega_{S/B}}]_S\{\omega_S\} + [I]_S^{-1}(\{M_{A,T}\}_S - [\Omega_{\omega_S}]_S([I]_S\{\omega_S\})), \tag{A.3}$$

where $\{\omega_S\} = [P_S\ \ Q\ \ R_S]^T$ represents the angular velocity vector expressed in the stability reference frame, $[I]_S$ is the stability–axes inertia matrix and $\{M_{A,T}\}_S$ are aerodynamic and propulsive moments, respectively. The terms $[\Omega_{\omega_{S/B}}]_S$ and $[\Omega_{\omega_S}]_S$ represent the cross-product matrices of the angular velocity vector between stability and body axes $\{\omega_{S/B}\} = [0\ \ -\dot{\alpha}\ \ 0]^T$ and the angular velocity vector of the stability reference frame $\{\omega_S\}$, respectively.

The vehicle attitude is modeled by the Euler kinematical relations

$$\{\dot{\Phi}\} = [T_{VA}]\{\omega_B\}, \tag{A.4}$$

where $\{\Phi\} = [\phi\ \ \theta\ \ \psi]^T$ is the Euler angles vector, consisting of roll, pitch and yaw angles, respectively. The transformation matrix $[T_{VA}]$ denotes the kinematical relationship between Euler angles and angular velocity components.

The navigation equations for trajectory evaluation are

$$\{\dot{p}\} = [T_{VW}]\{V_E\}_W, \tag{A.5}$$

where the position vector $\{p\} = [X_V\ \ Y_V\ \ Z_V]^T$ represents the center of gravity coordinates in a local navigation reference frame.

The aerodynamic and propulsive control commands are represented by elevon deflection η_{el} and throttle input τ, respectively.

The elevon surfaces perform as ailerons, whenever an antisymmetric deflection is operated, and as elevator, whenever a symmetric deflection is operated. Elevon deflections enter into the aerodynamic model determining, together with the aircraft states, the aerodynamic loads F_A and M_A. This dependence is taken into account by the following formulas:

$$F = \tfrac{1}{2}\varrho V^2 S C_F(\alpha,\beta,\eta_{el}), \quad M = \tfrac{1}{2}\varrho V^2 S l C_M(\alpha,\beta,\eta_{el}), \tag{A.6}$$

where flight conditions are represented by the atmospheric density ϱ and flight speed V, aircraft geometry is given by the wing surface S and the reference length l. The dimensionless coefficients C_F and C_M, referring to forces and moments, respectively, can be expressed in the general form (see Stevens & Lewis, 2003):

$$C_F = C_F(\alpha,\beta) + \Delta C_F(\eta_{el}), \quad C_M = C_M(\alpha,\beta) + \Delta C_M(\eta_{el}) + \frac{l}{2V}C_{M_\pi}. \tag{A.7}$$

The first term in Eq. (A.7) introduces dependence on aerodynamic angles while the second term refers to aerodynamic load increments due to control surfaces deflection. The third term in the moment dimensionless coefficient equation represents the dynamic derivatives, i.e. the effects of angular rates (generally indicated as π). The effects of control surfaces deflection are linearized around the equilibrium condition, introducing the aerodynamic control derivatives C_{F_η} and C_{M_η}:

$$\Delta C_F(\eta_{el}) = \frac{\partial C_F}{\partial \eta_{el}}\eta_{el} = C_{F_\eta}\eta_{el}, \quad \Delta C_M(\eta_{el}) = \frac{\partial C_M}{\partial \eta_{el}}\eta_{el} = C_{M_\eta}\eta_{el}. \tag{A.8}$$

It is worth to note that the aerodynamic control derivatives, as well as the dynamic derivatives, are treated as uncertain parameters within the proposed methodology (see Section 4).

Linear relationships modeling a DC motor-based propulsion and classical blade element theory are used to compute propulsive forces F_T and moments M_T as a function of the throttle input (see, e.g. McCormick, 1995).

The state-space formulation used for control synthesis and analysis is obtained by numerical linearization of the full order system about an equilibrium condition.

Appendix B. Meta-algorithms

Algorithm 1 (*Random gain synthesis—RGS*). *Given* $\varepsilon,\eta \in (0,1)$, *the algorithm returns the set of gains* $\{K^1,K^2,\ldots,K^s\}$ *satisfying the specification* $\mathscr{S}_{RGS}$.

1: Compute N_K using the Log-over-log Bound;
2: Set $s = 0$;
3: For fixed $j = 1,2,\ldots,N_K$, generate uniformly the gain random matrix $K^j \in \mathscr{B}_K$;

4: For fixed $i = 1, 2, \ldots, M$, compute the closed-loop matrix $A_{cl}^i(K^j) = A_c^i - B_c^i K^j$;
- if K^j does not satisfy $\mathscr{S}_{RGS}$, go to Step 7;
5: End;
6: Set $s = s + 1$ and return the gain K^j;
7: Set $j = j + 1$ and return to Step 3;
8: End.

Algorithm 2 (*Pole placement—PP*). *Given the dynamic characteristics in terms of natural frequency and damping ratio, returns the gain matrix K^{PP} satisfying the desired dynamics.*

1: Check controllability of the system $\dot{x}(t) = Ax(t) + Bu(t)$;
2: Write the system in controllable canonical form using the transformation $x(t) = Tz(t)$ obtaining $\dot{z}(t) = A^{con}z(t) + B^{con}u(t)$;
3: Choose a set of desired eigenvalues $\lambda_1^{des} \cdots \lambda_n^{des}$ and write the desired characteristic equation $\prod_{i=1}^{n}(s - \lambda_i^{des}) = s^n + \alpha_{n-1}s^{n-1} + \cdots + \alpha_0$;
4: Return the gain matrix K^{PP} obtained equating $\det(sI - A^{con} + B^{con}K^{PP})$ with the desired characteristic equation;
5: End.

Algorithm 3 (*Random stability robustness analysis–RSRA*). *Given $\varepsilon, \eta \in (0, 1)$, the algorithm returns the empirical probability P_{RSRA} that the specification $\mathscr{S}_{RSRA}$ is satisfied for a gain matrix $\overline{K}$ provided either by Algorithm RGS or Algorithm PP.*

Compute N_Δ using the Chernoff Bound;
Generate N_Δ i.i.d. random vectors $\Delta^j \in \mathscr{B}_\Delta$ according to the given p.d.f.;
For fixed $j = 1, 2, \ldots, N_\Delta$, compute the closed-loop matrix $A_{cl}(\Delta^j) = A(\Delta^j) - B(\Delta^j)\overline{K}$;
- if $A_{cl}(\Delta^j)$ satisfies $\mathscr{S}_{RSRA}$, set $\mathscr{I}(\Delta^j) = 1$;
- otherwise, set $\mathscr{I}(\Delta^j) = 0$;
End;
Return the empirical probability $P_{RSRA} = (1/N_\Delta)\sum_{j=1}^{N_\Delta}\mathscr{I}(\Delta^j)$.

Algorithm 4 (*Random Performance Robustness Analysis–RPRA*). *Given N_Δ and $A_{cl}(\Delta^j)$, $j = 1, 2, \ldots, N_\Delta$, provided by Algorithm RSRA, the algorithm returns the empirical probability P_{RPRA} that the specification $\mathscr{S}_{RPRA}$ is satisfied for a gain matrix $\overline{K}$ provided either by Algorithm RGS or Algorithm PP.*

For $j = 1, 2, \ldots, N_\Delta$
- if $A_{cl}(\Delta^j)$ satisfies $\mathscr{S}_{RPRA}$, set $\mathscr{I}(\Delta^j) = 1$;
- otherwise, set $\mathscr{I}(\Delta^j) = 0$;
End;
Return the empirical probability $P_{RPRA} = (1/N_\Delta)\sum_{j=1}^{N_\Delta}\mathscr{I}(\Delta^j)$.

References

Anonymous (1997). Flying qualities of piloted aircraft. MIL-HDBK-1797, Department of Defense, USA.

Barmish, B. R. (1994). *New tools for robustness of linear systems*. New York: Macmillan.

Campa, G., Gu, Y., Seanor, B., Napolitano, M. R., Pollini, L., & Fravolini, M. L. (2007). Design and flight-testing of non-linear formation control laws. *Control Engineering Practice*, *15*, 1077–1092.

Chernoff, H. (1952). A measure of asymptotic efficiency for tests of a hypothesis based on the sum of observations. *Annals of Mathematical Statistics*, *23*, 493–507.

Davis, W. R. (1996). MicroUAVs. In *23rd Annual AUVSI Symposium*.

Dobrokhodov, V. N., Kaminer, I. I., Jones, K. D., & Reza, G. (2006). Vision-based tracking and position estimation for moving targets using small UAVs. In *Proceedings of the American control conference*, Minneapolis.

Elgersma, M., Ganguli, S., Ha, V., & Samad, T. (2004). Statistical performance verification for an autonomous rotorcraft. In *Proceedings of the IEEE international symposium on intelligent control*, Taipei, Taiwan.

Etkin, B. (2003). *Dynamics of atmospheric flight*. New York: Wiley.

Fujisaki, Y., Dabbene, F., & Tempo, R. (2003). Probabilistic robust design of LPV control systems. *Automatica*, *39*, 1323–1337.

Fujisaki, Y., Oishi, Y., & Tempo, R. (2008). Mixed deterministic/randomized methods for fixed order controller design. *IEEE Transactions on Automatic Control*, *53*, 2033–2047.

Keviczky, T., & Balas, G. J. (2005). Flight test of a receding horizon controller for autonomous UAV guidance. In *Proceedings of the American control conference*, Portland.

Lombaerts, T. J. J., Mulder, J. A., Voorsluijs, G. M., & Decupyere, R. (2005). Design of a robust flight control system for a Mini-UAV. In *Proceedings of AIAA guidance, navigation, and control conference and exhibit*, San Francisco.

Lu, B., & Wu, F. (2006). Probabilistic robust linear parameter-varying control of an F-16 aircraft. *Journal of Guidance, Control and Dynamics*, *29*, 1454–1460.

Marrison, C. I., & Stengel, R. F. (1997). Robust control system design using random search and genetic algorithms. *IEEE Transactions on Automatic Control*, *42*, 835–839.

McCormick, B. (1995). *Aerodynamics, aeronautics and flight mechanics*. New York: Wiley.

Ogata, K. (1995). State space—pole placement. In: *The Control Handbook*. Boca Raton: CRC Press, pp. 209–215.

Peddle, I. K., Jones, T., & Treurnicht, J. (2009). Practical near hover flight control of a ducted fan (SLADe). *Control Engineering Practice*, *17*, 48–58.

Pralio, B., Guglieri, G., & Quagliotti, F. (2003). Design and performance analysis of a microaerial vehicle concept. In *Proceedings of the AIAA "unmanned unlimited" systems technologies, and operations—aerospace, land and sea conference*, San Diego.

Ray, L. R., & Stengel, R. F. (1992). Stochastic measures of performance robustness in aircraft control systems. *Journal of Guidance, Control, and Dynamics*, *15*, 1381–1387.

Ray, L. R., & Stengel, R. F. (1993). A Monte Carlo approach to the analysis of control system robustness. *Automatica*, *29*, 229–236.

Redding, J. D., McLain, T. W., Beard, R. W., & Taylor, C. N. (2006). Vision-based target localization from a fixed-wing miniature air vehicle. In *Proceedings of the American control conference*, Minneapolis.

Sanna, A., & Pralio, B. (2005). Innovative tool for simulating and controlling mini air vehicles. *WSEAS Transactions on Information Science and Applications*, *2*, 1659–1666.

Stengel, R. F. (1980). Some effects of parameter variations on the lateral-directional stability of aircraft. *AIAA Journal of Guidance and Control*, *3*, 124–131.

Stevens, B. L., & Lewis, F. L. (2003). *Aircraft control and simulation*. New York: Wiley.

Tempo, R., Bai, E. W., & Dabbene, F. (1997). Probabilistic robustness analysis: Explicit bounds for the minimum number of samples. *Systems & Control Letters*, *30*, 237–242.

Tempo, R., Calafiore, G., & Dabbene, F. (2005). *Randomized algorithms for analysis and control of uncertain systems*. London: Springer.

Vidyasagar, M. (1998). Statistical learning theory and randomized algorithms for control. *IEEE Control Systems Magazine*, *18*, 69–85.

Vidyasagar, M., & Blondel, V. (2001). Probabilistic solutions to some NP-hard matrix problems. *Automatica*, *37*, 1397–1405.

Wang, Q., & Stengel, R. F. (2005). Robust nonlinear flight control of a high performance aircraft. *IEEE Transactions on Control Systems Technology*, *13*, 15–26.

Wang, Q., & Stengel, R. F. (2006). Probabilistic control of nonlinear uncertain dynamic systems. In *Probabilistic and randomized methods for design under uncertainty*. London: Springer, pp. 381–414.

Zhou, K., Doyle, J. C., & Glover, K. (1996). *Robust and optimal control*. Upper Saddle River: Prentice-Hall.